Electronic Supplementary Information

ESI.1 Experimental Section

Compound 1. $[H_2N(C_2H_4)_2NH_2]_{1.5}[(VO)_2(AsO_4)F_2]O[(VO)(HAsO_4)F].H_2O$ (1): Vanadium(V) oxide (0.1046 g, 0.575 mmol), 85% orthoarsenic acid solution (0.04 mL, 0.575 mmol), 48% hydrofluoric acid solution (0.05 mL, 1.38 mmol), piperazine (0.0991 g, 1.15 mmol) and distilled water (3 mL, 166.6 mmol) were mixed in the Teflon® liner of a Parr 23 ml hydrothermal vessel; the final reaction mixture pH was 5.24. The hydrothermal vessel was sealed and heated to 418 K for 4 days. The pure solid product formed as very dark blue crystals and was isolated by filtration, washed with distilled water and dried at 60°C. SEM/EDAX analysis (ESI.10) gave V:As ratio of 1.55:1; theoretical 1.5:1. Crystal data $C_6H_{21}As_2F_3N_3O_{13}V_3$ (M_r =702.92), triclinic, P-1, a=8.5594(2), b=10.8001(2), c=12.0616(2)Å, α=65.592(1)° β=79.893(1)° γ=72.065(1)°, V= 964.51(3) Å^3, *Z=2*, ρ_{calcd}=2.420 gcm^{-3}, μ = 4.926mm^{-1}, $Mo_{K\alpha}$ λ=0.71073 Å, T=120(2) K , ϑ_{max}=27.48°, *R_1=0.0291, wR_2=0.0621.* CCDC 812051.

Compound 2. $[H_2N(C_2H_4)_2NH_2]_{1.5}[(VO)_3(AsO_4)F_4][VF_3(AsO_4)].4H_2O$ (2): Reaction method as for compound (1). Vanadium(V) oxide (0.1046 g, 0.575 mmol), 85% orthoarsenic acid solution (0.04 mL, 0.575 mmol), 48% hydrofluoric acid solution (0.1 mL, 2.76 mmol), piperazine (0.0991 g, 1.15 mmol) and distilled water (3mL, 166.6 mmol). The reaction mixture had a pH value = 3.28. The single phase product crystallized as dark green plates. SEM/EDAX analysis (ESI.10) gave V:As ratio of 1.85:1; theoretical 2:1. Crystal data $C_6H_{26}As_2F_7N_3O_{15}V_4$ (M_r =866.9), monoclinic, $P2_1/c$, a=16.8763(6), b=14.1659(5) c=10.7198(4)Å, β= 93.894(2), V= 2556.84(16) Å^3, *Z=4*, ρ_{calcd}=2.252gcm^{-3}, μ = 4.104mm^{-1}, $Mo_{K\alpha}$ λ=0.71073 Å, T=120(2) K , ϑ_{max}=25.03°, *R_1=0.0676(3388 reflections), wR_2=0.1845(4513 reflections)*. CCDC 812052.

Compound 3. $[H\text{-}DABCO]_xV_{72}As_{24}O_{204}F_{54}.nH_2O$ (3): Reaction method as for compound (1). Vanadium (III) fluoride (0.0621 g, 0.575 mmol) was combined with 70% orthoarsenic acid solution (0.06 mL, 0.575 mmol), dabco (0.0645 g 0.575 mmol) and distilled water (4 mL, 222.2 mmol). Heated to 418 K for 4 days. Single phase product of green needles, see SI. SEM/EDAX analysis (ESI.10) gave V:As:O/F ratio of 2.63:1; theoretical 3:1. Crystal data $As_{12}F_{27}O_{99.69}V_{36}$ (M_r =4840.92), hexagonal, $P6_3/m$, a=32.3426(8) c=10.6928(4)Å, V= 9686.6(5) Å^3, *Z=2*, ρ_{calcd}=1.678gcm^{-3}, μ = 3.770mm^{-1}, $Mo_{K\alpha}$ λ=0.71073 Å, T=120(2) K , ϑ_{max}=25.03°, *R_1=0.1006(2644 reflections), wR_2=0.2950(6027 reflections)*. Disordered solvent and template molecules and their contribution to the scattering were removed using PLATON SQUEEZE[15] . CSD 422649.

ESI .2. Structure refinement details.

For all compounds cell dimensions and intensity data were recorded at 120K, using a Bruker Nonius APEXII (**1,3**) or KappaCCD Roper (**2**) area detector diffractometer mounted at the window of a rotating Mo anode (λ(Mo-Kα) = 0.71073Å) operating at 50KV, 85mA. The incident beam on the APEXII side was focused using 10cm confocal mirrors, a graphite monochromator was employed on the KappaCCD side. The crystal-to-detector distance was 30mm for **1,2** and 45mm for **3.** ϕ and ω scans were carried out to fill the asymmetric unit using 2° frames and 20s per frame exposures for **1,** 2° and 140s for **2** and 1.1° and 71s for **3**. Unit cell determination, data collection and processing were carried out using the programs DirAx[1], COLLECT[2] and DENZO[3] and a multi-scan absorption correction was applied using SADABS[4].

The structures were solved via direct methods[5] and refined by full matrix least squares[5] on F^2.

Refinement procedure for 1: The hydrogen atoms of the protonated piperazine (the second of which lies on an inversion centre) were all clearly located in the difference map and subsequently placed in idealized positions and treated using a riding model approximation with U(H) fixed at 1.2Ueq of the parent atom. The coordinates for hydrogen atoms of the water OW1 and the hydroxyl hydrogen of O6 were obtained from the difference map and subsequently treated as riding on the parent atom, the U(iso) values were freely refined. Oxygen and fluorine sites were clearly identifiable and distinguishable on the basis of their electron density during the refinement process (e.g. ADPs of sites wrongly assigned as O became non-positive definite); subsequent bond-valance sums (see Section ESI 3) for the anion distributions confirmed the distribution.

Refinement procedure for 2: 6 sites were identified as probable water molecules and due to several close contacts and elevated thermal parameters the following approach to refinement was adopted. A global anisotropic temperature factor was applied and the occupancies allowed to refine, this identified 2 sites (O1W and O2W) as fully occupied with the remainder being partially occupied – these occupancies were subsequently fixed as 0.5. Whilst there are numerous electron density peaks at suitable distances from these water oxygens no attempt was made to interpret the hydrogen bonding network or to refine hydrogen positions – the appropriate number of inferred hydrogens was included in the model formula. The hydrogen atoms of the protonated piperazine (the second of which lies on an inversion centre) were all clearly located in the difference map and subsequently placed in idealized positions and treated using a riding model approximation with U(H) fixed at 1.2Ueq of the parent atom. Oxygen and fluorine sites were clearly identifiable and distinguishable as for compound (**1**)

---

[1] Duisenberg AJM. Indexing in Single-Crystal Diffractometry with an Obstinate List of Reflections. *Journal of Applied Crystallography* 1992; **25**: 92-96.
[2] COLLECT data collection software, Nonius B.V., 1998.
[3] Z. Otwinowski and W. Minor, " Processing of X-ray Diffraction Data Collected in Oscillation Mode ", Methods in Enzymology, Volume 276: Macromolecular Crystallography, part A, p.307-326, 1997,C.W. Carter, Jr. & R.M. Sweet, Eds., Academic Press.
[4] Sheldrick, G. M. SADABS - Bruker Nonius area detector scaling and absorption correction - V2.10
[5] SHELX97: Programs for Crystal Structure Analysis (Release 97-2). G. M. Sheldrick, Institüt für Anorganische Chemie der Universität, Tammanstrasse 4, D-3400 Göttingen, Germany, 1998.

Refinement procedure for 3: The data collection and refinement of this structure presented several challenges whose root causes lie in the inherently disordered nature of the 'straw like' structure. In an attempt to get the best possible data many (~10) data sets were collected on many different crystals, both on a high power lab source and a synchrotron source (Diamond). However, these data sets and subsequent refinements were all very similar; we present the best refinement obtainable. The first question was that of space-group; the merging R statistics were very high for all Bravais lattices, but significantly lower for monoclinic P and hexagonal P. This in combination with systematic absences for a 6_3 screw and an E2-1 value tending towards centrosymmetric suggested a space-group of $P6_3/m$, and after many trial refinements this was chosen as the final symmetry for this structure. The non centro symmetric $P6_3$ was rejected due to apparent correlation between thermal parameters related by the mirror plane of $P6_3/m$. The monoclinic refinement twinned to emulate hexagonal was also tried without success.

The second challenge was the elucidation of the contents of the large channel, this in conjunction with smaller void space between 'tubes' presents a potential solvent accessible void of 4916.6Å^3. Analysis of difference electron density maps of the large channel showed a pattern of discrete peaks adjacent to the inward facing surface of the framework, Fig S5.1a. These were interpreted as the average electron density of a partially occupied VO_n groups that is present at an occupancy of ~0.5. The highest electron density peaks were refined as partial V's (V6A,V6B,V6C and V6D) with linked thermal parameters, the refined occupancies were close to 0.5 and subsequently fixed as such. These sites were not assigned to arsenic as the electron density was too low and occupancy by As would require the formation of pyroarsenate, As_2O_7 , units a feature not seen elsewhere in this work; however such a possibly cannot be totally discounted.

Several areas of electron density associated with possible oxygen positions coordinated to V6(A-D) sites were located in difference Fourier maps and oxygen assigned to these positions (OX1-OX10) and 8 of these sites incorporated in the final refinement with low (refined) occupancies (note that these sites may also be fluorine – *vide infra*) . In addition to the poorly defined oxygens atoms associated with the V6 positions there is likely to be considerable solvent/template/free arsenate anion density thinly smeared through the large channel and spaces between 'tubes'. This hypothesis was tested by employing the SQUEEZE[6] algorithm that gave a tentative value of 2059 electrons per cell and significantly reduced the R-factor.

Oxygen and fluorine sites were clearly identifiable and distinguishable for the non-disordered section of the structure – as for compound (**1**). Disorder within the polyhedra centred on V6(A-D) makes definitive assignment of the anion sites impossible and the composition of these units is reported as $[V_4(O,F)_4]_{½}\}_{12}$

The authors are satisfied that the refinement is a true representation of the majority of the structure, but there remains some ambiguity over the exact nature of the internal surface of the channels and their solvent content.

[6] Sluis, P. v.d.; Spek, A. L. Acta Crystallogr., Sect A 1990, 46, 194-201.

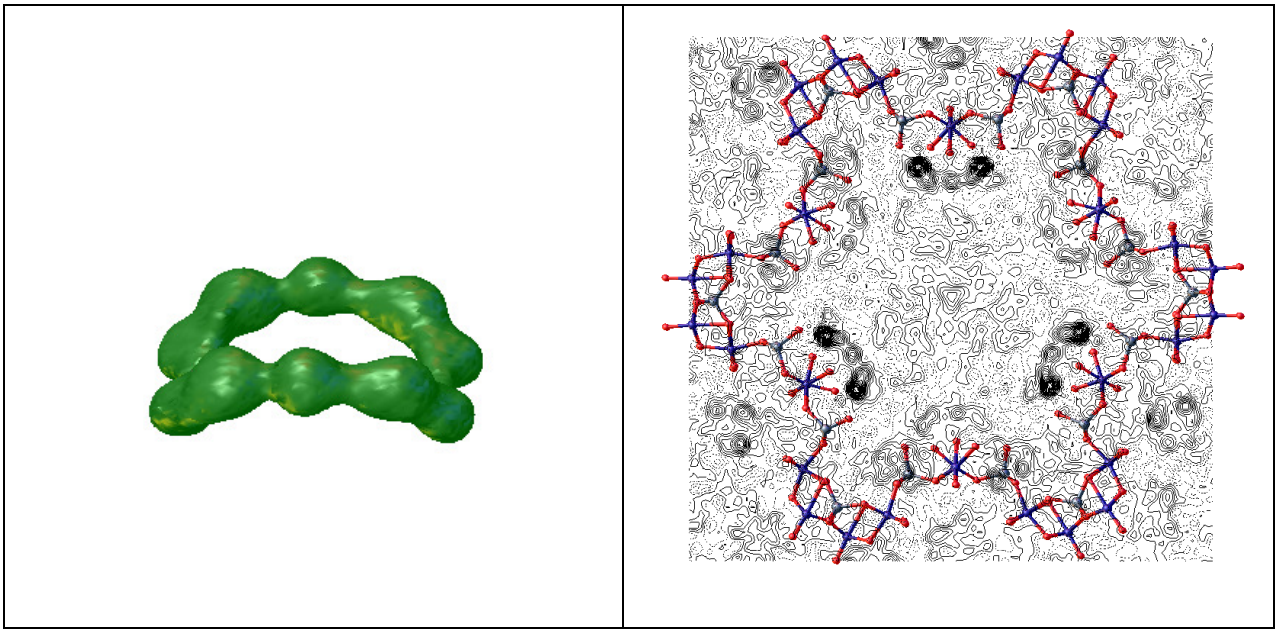

(a) (b)

SI1.a (a) Plot of the electron density distribution that is located on the face of an inward pointing VO_6 octahedra, and is interpreted as the average V distribution representing by additional positionally disordered octahedra whose oxygen atoms are too diffuse to be visible. (b) Difference electron density slice through the channel showing the localized density depicted in (a) and the diffuse density within the centre of the channel. Due to the screw axis at the centre of the channel only every other disordered site is visible in this particular slice.

ESI.3 Compound (**1**). Additional structural diagrams and bond valence calculations.

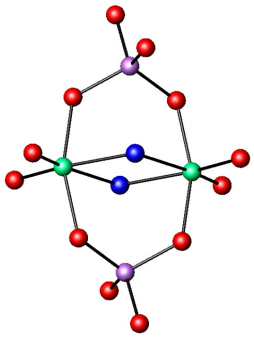

Schematic showing the $V_2O_8F_2$ dioctahedral units identified in compound (**1**) for V(1), V(2) and V(3).

The three different dioctahedral units present in compound (**1**) with interatomic distances shown. From top to bottom V1(vanadium(5+)), V2(vanadium (4+)) and V3 (vanadium (4+))

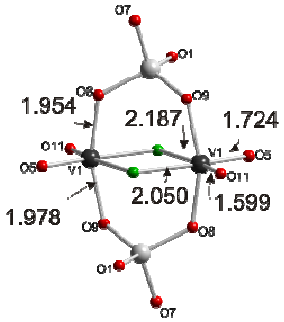

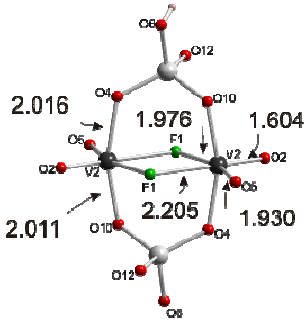

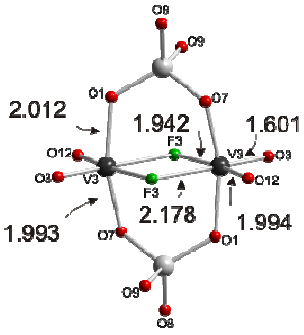

Selected bond lengths (Å) and bond valences for compound **(1)**.

Polyhedra	**Bond lengths**	**Σs_{ij}**	**Polyhedra**	**Bond lengths**	**Σs_{ij}**
$V(1)O_4F_2$			**$V(3)O_4F_2$**		
V(1)-O(5)	*1.724(3)*	1.238	V(3)-O(1)	2.012(3)	0.540
V(1)-O(8)	1.954(3)	0.665	V(3)-O(3)	1.601(3)	1.640
V(1)-O(9)	1.978(3)	0.623	V(3)-O(7)	1.993(3)	0.568
V(1)-O(11)	1.599(3)	1.736	V(3)-O(12)	1.994(3)	0.567
V(1)-F(2)	2.050(3)	0.388	V(3)-F(3)	1.942(3)	0.520
V(1)-F(2')	2.187(3)	0.268	V(3)-F(3')	2.178(3)	0.275
		ΣV1=4.92			**ΣV3=4.11**
$V(2)O_4F_2$			**$As(1)O_4$**		
V(2)-O(2)	1.604(3)	1.627	As(1)-O(1)	1.685(3)	1.248
V(2)-O(4)	2.016(3)	0.534	As(1)-O(7)	1.700(2)	1.199
V(2)-O(5)	1.930(3)	0.674	As(1)-O(8)	1.697(2)	1.208
V(2)-O(10)	2.011(3)	0.541	As(1)-O(9)	1.693(3)	1.221
V(2)-F(1)	1.976(3)	0.474			**ΣAs1=4.88**
V(2)-F(1')	2.205(3)	0.256			
		ΣV2=4.10	**$HAs(2)O_4$**		
			As(2)-O(4)	1.681(3)	1.262
			As(2)-O(6)	1.720(3)	1.135
			As(2)-O(10)	1.693(3)	1.221
			As(2)-O(12)	1.665(3)	1.317
					ΣAs2=4.94

ESI.4 Compound (**2**). Additional structural diagrams and bond valence calculations.

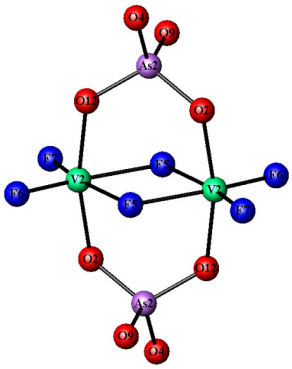

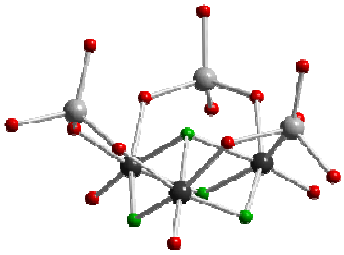

Schematic showing parts of the building units identified in compound (**2**): $[V_2As_2O_8F_6]^{4-}$ unit (top left) and (right) the $[(VO)_3F_4(AsO_4)_{1+2/2}]^{4-}$ ball and stick (top) and polyhedral (bottom) representations.

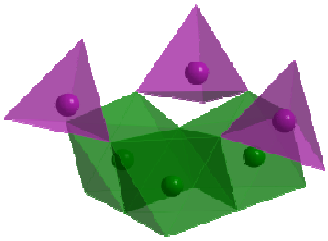

Connectivity of building units in compound (**2**) . The $[(VO)_3F_4(AsO_4)_{1+2/2}]$ units link through two arsenate groups, $(AsO_4)_{2/2}$ to form chains (top left) and then through the remaining arsenate groups to the $[V_2As_2O_8F_6]^{4-}$ unit (right, viewed at two almost perpendicular directions)

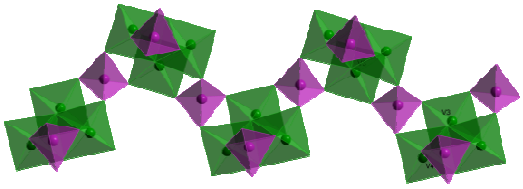

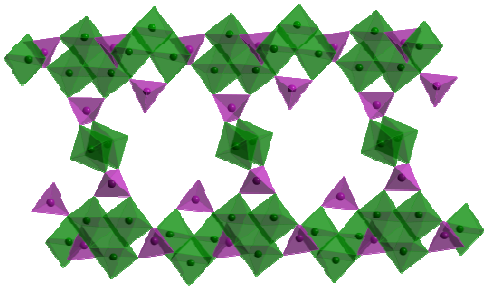

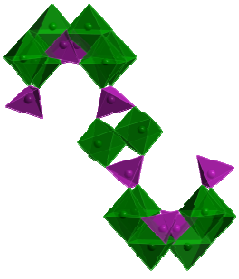

Selected bond lengths (Å) and bond valences for compound **(2)**.

Polyhedra	**Bond lengths**	**Σs_{ij}**	**Polyhedra**	**Bond lengths**	**Σs_{ij}**
$V(1)O_3F_3$			**$V(4)O_3F_3$**		
V(1)-O(3)	*1.619(7)*	1.562	V(4)-O(4)	1.964(7)	0.615
V(1)-O(9)	1.968(7)	0.608	V(4)-O(8)	1.989(6)	0.575
V(1)-O(11)	1.971(7)	0.603	V(4)-O(10)	1.608(7)	1.609
V(1)-F(2)	2.000(7)	0.445	V(4)-F(1)	2.027(6)	0.413
V(1)-F(3)	2.005(7)	0.439	V(4)-F(2)	1.985(6)	0.463
V(1)-F(4)	2.198(5)	0.260	V(4)-F(3)	2.169(5)	0.282
		ΣV1=3.92			**ΣV3=3.96**
$V(2)O_2F_4$			**$As(1)O_4$**		
V(2)-O(2)	1.974(7)	0.598	As(1)-O(5)	1.700(6)	1.199
V(2)-O(12)	1.985(7)	0.581	As(1)-O(7)	1.688(6)	1.238
V(2)-F(5)	2.041(6)	0.398	As(1)-O(8)	1.703(6)	1.189
V(2)-F(5')	2.102(6)	0.337	As(1)-O(11)	1.674(6)	1.286
V(2)-F(6)	1.709(9)	0.976			**ΣAs1=4.91**
V(2)-F(7)	1.763(9)	0.843			
		ΣV2=3.73	**$As(2)O_4$**		
			As(2)-O(2)	1.693(7)	1.221
$V(3)O_3F_3$			As(2)-O(4)	1.688(6)	1.238
V(3)-O(5)	1.976(6)	0.595	As(2)-O(9)	1.681(6)	1.262
V(3)-O(6)	1.619(7)	1.562	As(2)-O(12)	1.688(7)	1.238
V(3)-O(7)	1.973(7)	0.600			**ΣAs2=4.96**
V(3)-F(1)	1.991(6)	0.455			
V(3)-F(3)	2.123(5)	0.319			
V(3)-F(4)	2.003(7)	0.441			
		ΣV3=3.97			

ESI.5 Compound (3). Additional structural diagrams and bond valence calculations.

Construction of the "tubes". Ordered VO_n polyhedra in purple, disordered $V(6)O_n$ polyhedra in cream and arsenate tetrahedral in purple. The "exo" (to the tube) polyhedral units shown right are as in compound (2) and form identical chains by linking through arsenate (bottom). These are connected through the $[V_2O_8F]$ dioctahedral unit (left)

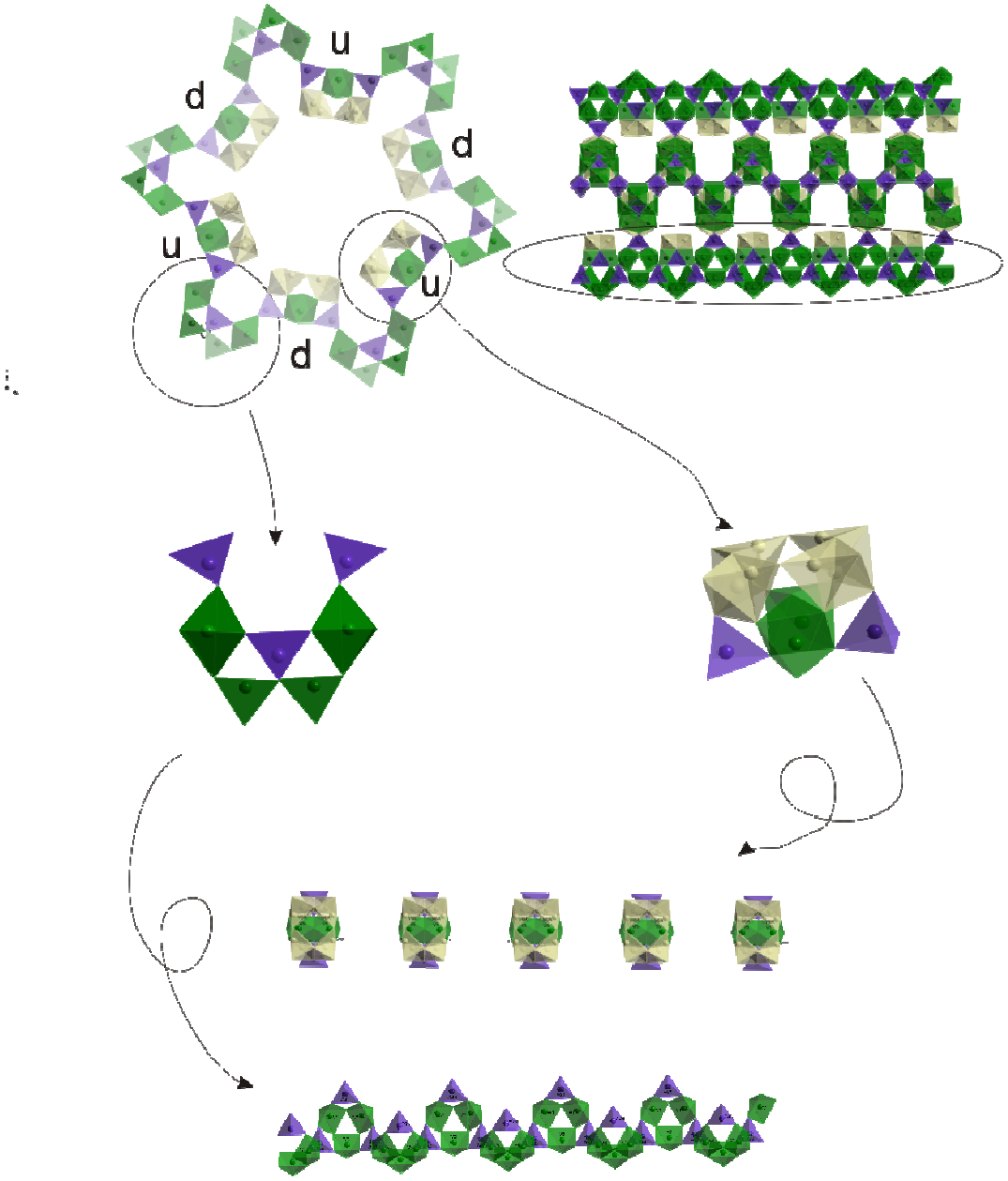

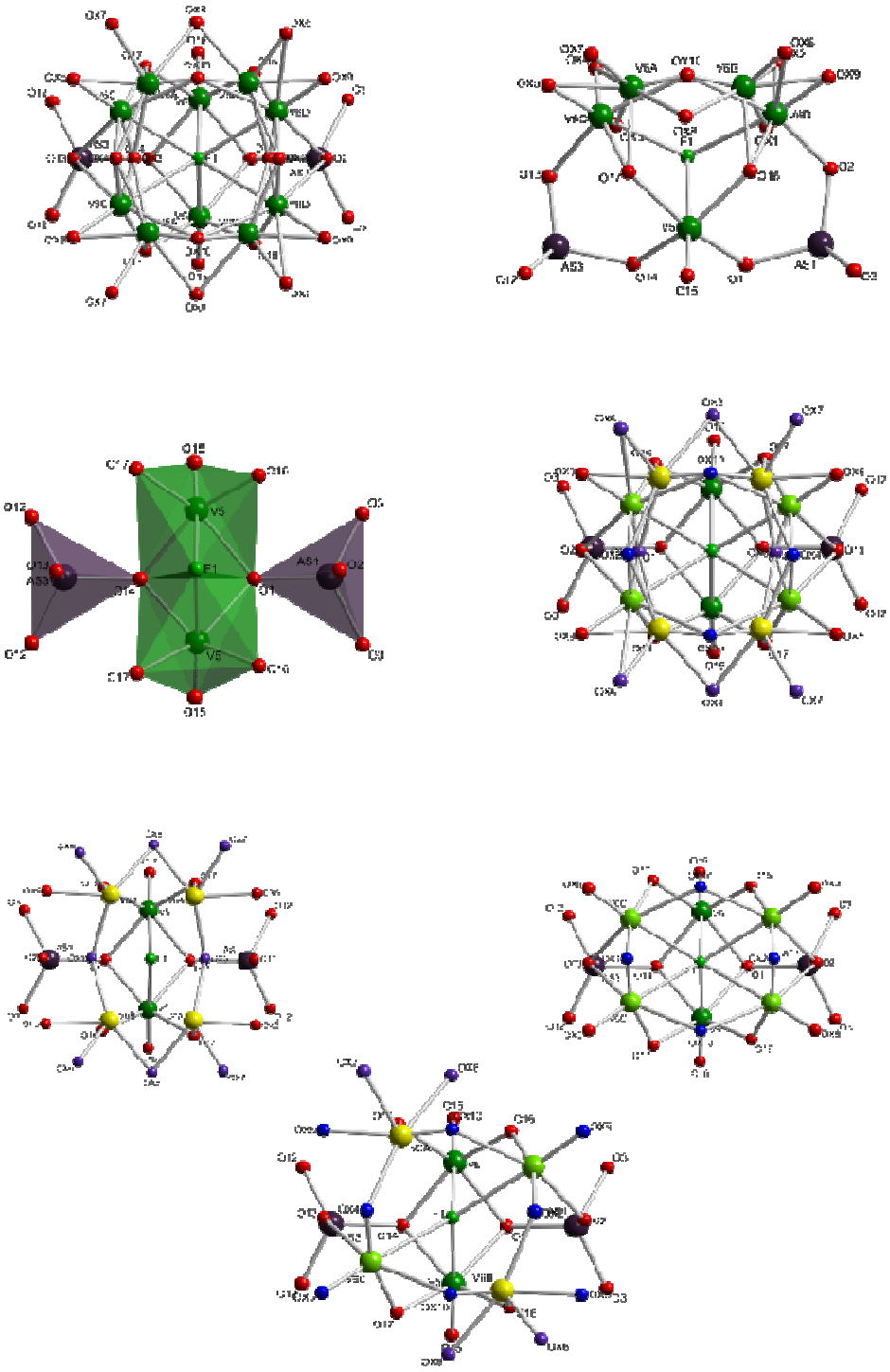

Possible models for the disordered capped $[V_2O_8F]$, V^{5+}, confacial dioctahedral unit (centre left). Upper diagrams show all refined atom positions. Lower diagram possible arrangements for vanadium and oxygen over the partially occupied sites giving a $[V_4O_4]_{½}$ unit with rectangular or skewed square geometries.

Selected bond lengths (Å) and bond valences for compound **(3)** for ordered sites

Polyhedra	Bond lengths	Σs_{ij}	Polyhedra	Bond lengths	Σs_{ij}
$V(1)O_3F_3$			**$V(4)O_3F_3$**		
V(1)-O(4)	*1.616(10)*	1.575	V(4)-O(11)	1.604(11)	1.627
V(1)-O(5)	1.937(10)	0.661	V(4)-O(9)	1.951(9)	0.637
V(1)-O(3)	1.981(11)	0.587	V(4)-O(12)	1.993(11)	0.568
V(1)-F(2)	1.861(6)	0.647	V(4)-F(5)	1.894(5)	0.592
V(1)-F(3)	1.934(9)	0.531	V(4)-F(7)	1.929(9)	0.539
V(1)-F(4)	2.181(7)	0.273	V(4)-F(6)	2.178(6)	0.275
		ΣV1=4.27			**ΣV3=4.24**
$V(2)O_3F_3$			**$V(5)O_5F$**		
V(2)-O(6)	1.621(14)	1.554	V(5)-O(15)	1.522(10)	2.137
V(2)-O(7)	1.940(9)	0.656	V(5)-O(16)	1.956(15)	0.661
V(2)-O(7')	1.940(9)	0.656	V(5)-O(17)	1.988(15)	0.607
V(2)-F(3)	1.903(8)	0.578	V(5)-O(14)	2.047(10)	0.517
V(2)-F(3')	1.903(8)	0.578	V(5)-O(1)	2.066(11)	0.491
V(2)-F(4)	2.238(12)	0.234	V(5)-F(1)	2.149(11)	0.297
		ΣV2=4.25			**ΣV5=4.71**
$V(3)O_3F_3$			**$As(2)O_4$**		
V(3)-O(10)	1.594(16)	1.759	As(2)-O(5)	1.660(11)	1.335
V(3)-O(8)	1.924(9)	0.721	As(2)-O(7)	1.693(9)	1.221
V(3)-O(8')	1.924(9)	0.721	As(2)-O(9)	1.698(11)	1.205
V(3)-F(7)	1.891(16)	0.597	As(2)-O(8)	1.704(9)	1.186
V(3)-F(7')	1.891(9)	0.597			**ΣAs2=4.95**
V(3)-F(6)	2.194(12)	0.263			
		ΣV3=4.66	**$As(3)O_4$**		
			As(3)-O(13)	1.661(20)	1.332
$As(1)O_4$			As(3)-O(12)	1.650(9)	1.372
As(1)-O(2)	1.670(21)	1.300	As(3)-O(12')	1.650(9)	1.372
As(1)-O(1)	1.707(12)	1.176	As(3)-O(14)	1.712(12)	1.160
As(1)-O(3)	1.711(11)	1.163			**ΣAs3=5.24**
As(1)-O(3')	1.711(11)	1.163			
		ΣAs1=4.80			

ESI.6 Optical images of Crystals of Compound (3) before and after heating under 5%H_2/N_2

ESI 6.1 Compound (**3**) as made

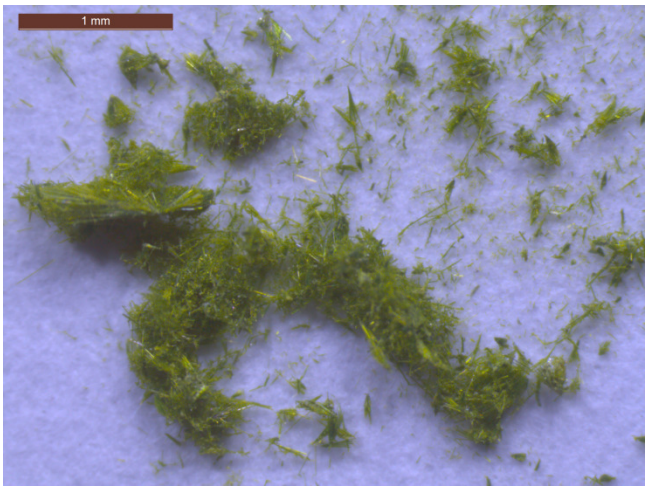

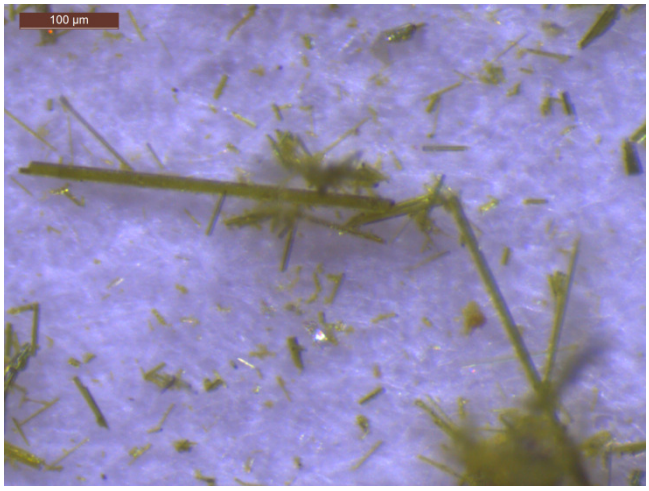

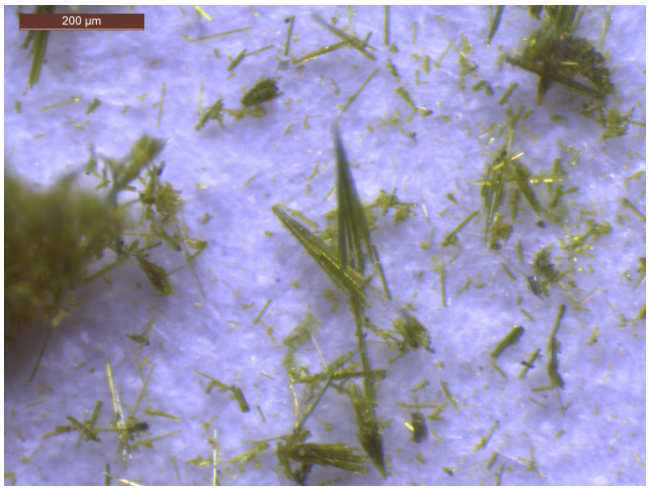

ESI6.2 Compound (**3**) after reduction at 400°C under 5% hydrogen in nitrogen

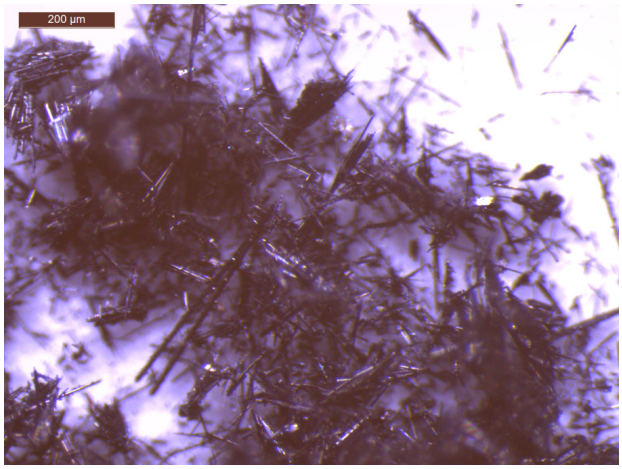

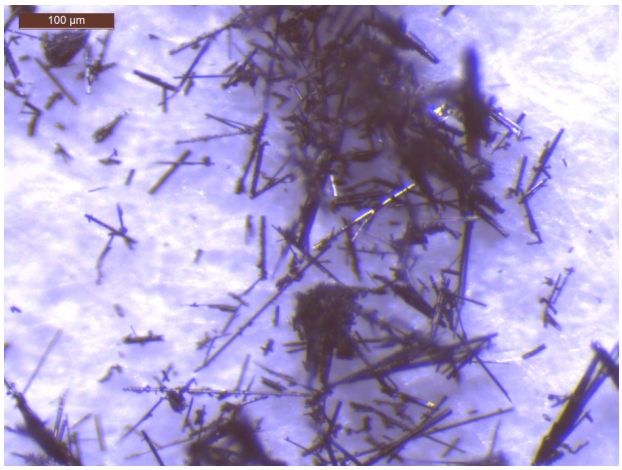

Compound (3) after reduction at 700°C under 5% hydrogen in nitrogen

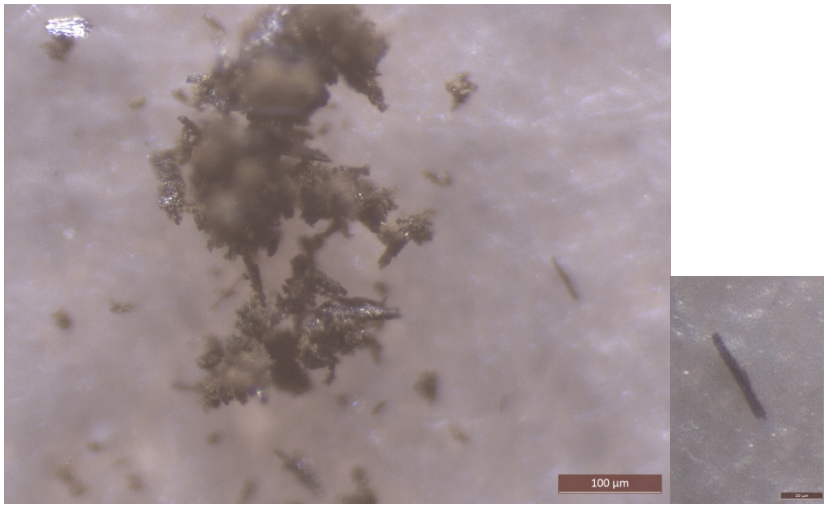

ESI.7 UV/Vis (Perkin-Elmer Lambda 35) diffuse reflectance spectra for compound (**1**) diluted 20 fold in KBr (upper spectra); for comparison with pure cavansite $Ca(VO)Si_4O_{10}(H_2O)_4$ (lower spectra) . Both spectra show absorption bands at ~850 nm assigned to the transitions d_{yz},d_{xz} to d_{xy} in V^{4+} . *Amoros, P.; Ibanez, R.; Martinez-Tamayo, E.; Beltran-Porter, A.; Beltran- Porter, D. Mater. Res. Bull.* ***1989****, 24, 1347.* Spectrum from compound 1 shows stronger absorption tail in UV/blue region and across the visible region associated with $V^{4+} \rightarrow V^{5+}$ transition.

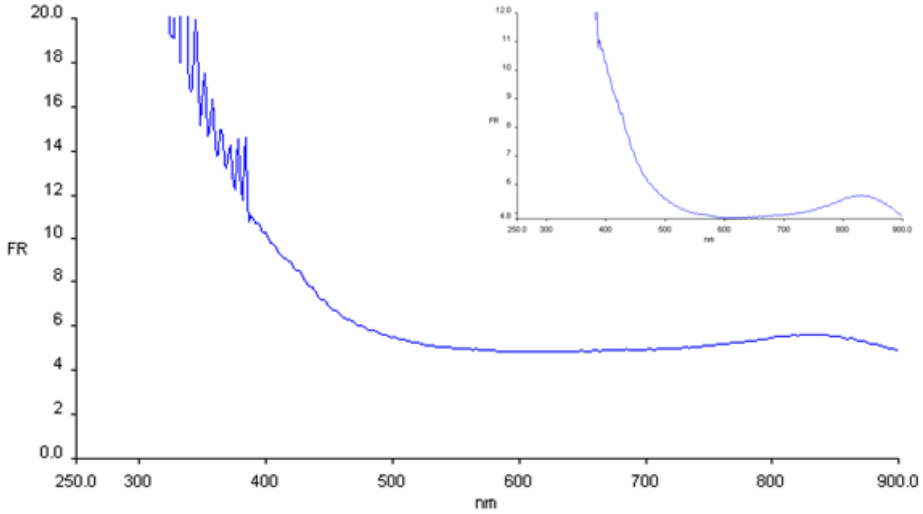

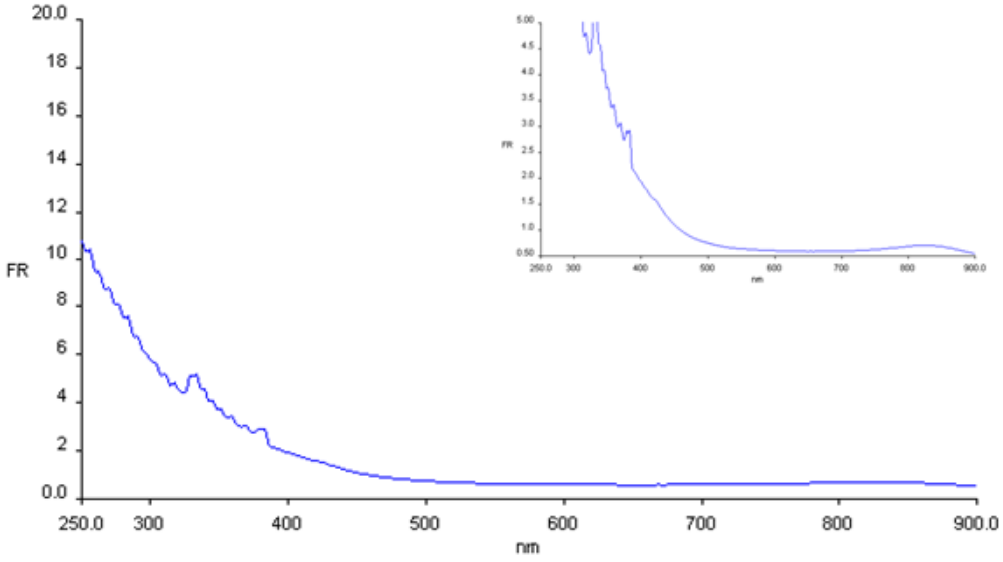

ESI.8 Thermogravimetric and Differential Thermal Analysis (DTA) data

ESI8.1 Combined TGA/DTA data from compound (**1**) heated in air at 20°C/min. Staged decomposition associated with water loss (endothermic, 1 molecule H_2O, 150-200°C), decomposition of piperazine (endothermic, 280°C) and framework collapse, loss of oxygen/water/HF/fluorine and formation of As(III) and V(IV) oxides (exothermic, 400-500°C)[T. Berrocal, J. L. Mesa, J. L. Pizarro, L. Lezama, B. Bazan, M. I. Arriortua and T. Rojo, *Journal of Solid State Chemistry* **2008**, *181*, 884-894.]

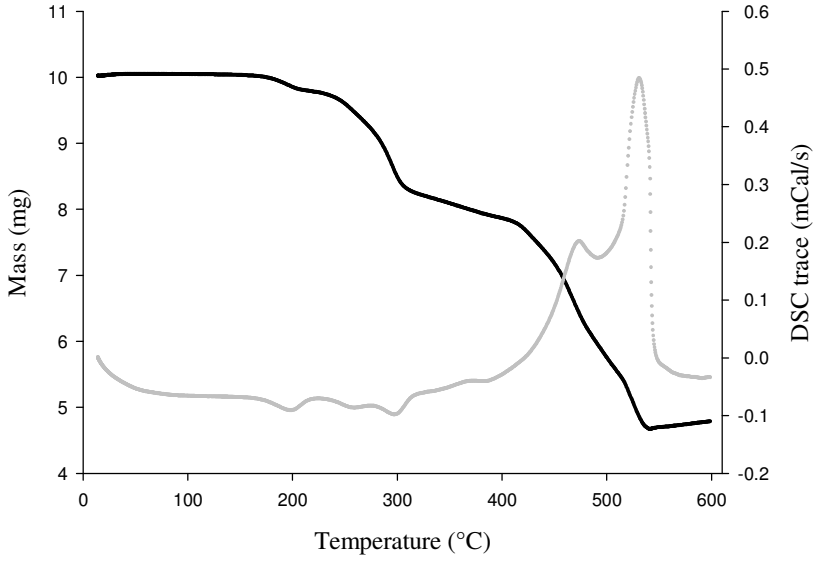

ESI8.2 Combined TGA/DTA data from compound (2) heated in air at 20°C/min. Staged decomposition associated with water loss (4 molecules H_2O 100-150°C), decomposition of piperazine (280-350 °C) and framework collapse, loss of oxygen/water/HF/fluorine and formation of As(III) and V(IV) oxides (450-500°C)

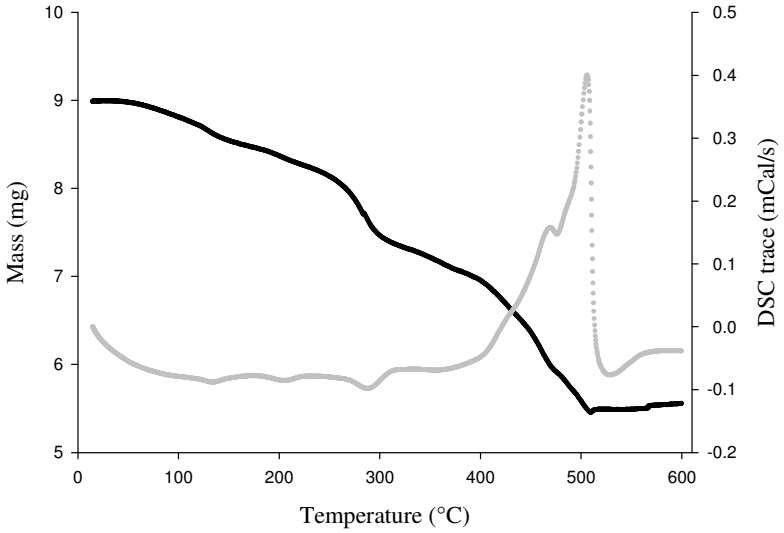

ESI8.3 Combined TGA/DTA data from compound (**3**) heated in air at 20 °C/min.

Staged decomposition associated with water loss (50-120°C), decomposition of Dabco (~250°C) and framework collapse, loss of oxygen/water/HF/fluorine and formation of As(III) and V(IV) oxides (450-500°C)

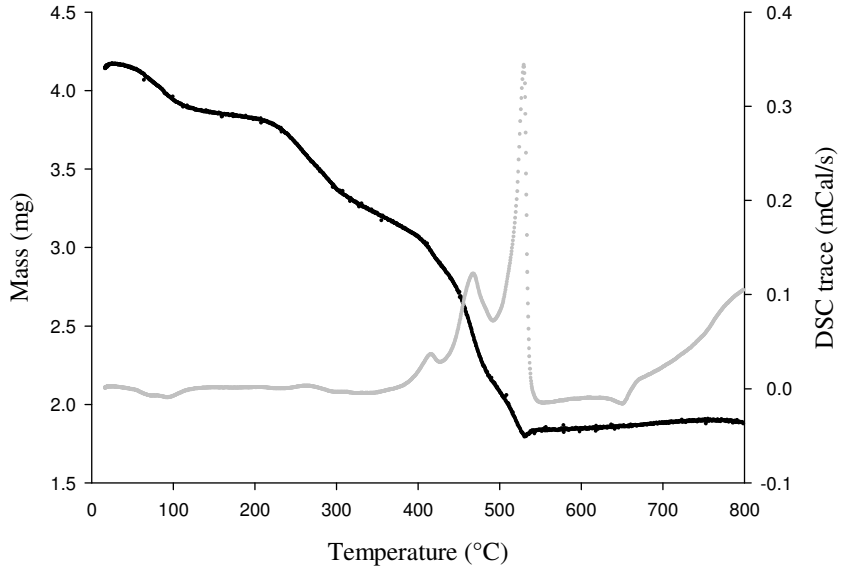

ESI8.4 Combined TGA/DSC data from 0.5mg of compound (**3**) heated under 5%H_2 in N_2. Staged decomposition associated with decomposition of dabco (250°C). Reduction occurs between 500 and 600 °C with framework collapse, loss of oxygen/water/HF.

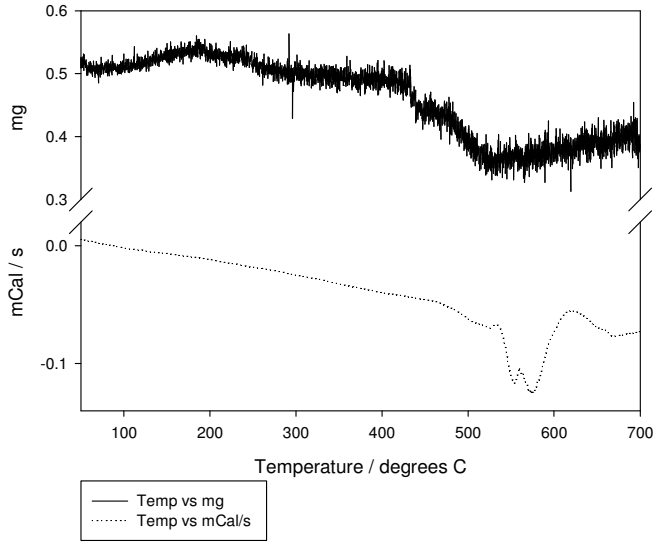

E**SI.9. Variable temperature PXD data from compound(3) from 30 – 160 °C**

Data (Cu Kα radiation, Siemens D8 PXD) plotted at 10°C intervals from 30-150 °C (top to bottom) for the showing the (220) and (310) reflections at 10.9° and 11.4°. Material contracts in the *ab* plane until ~70°C, presumably due to rearrangement of inter-tube solvent, and then expands only slowly to 150°C with associated water loss (see TGA data SI.8)

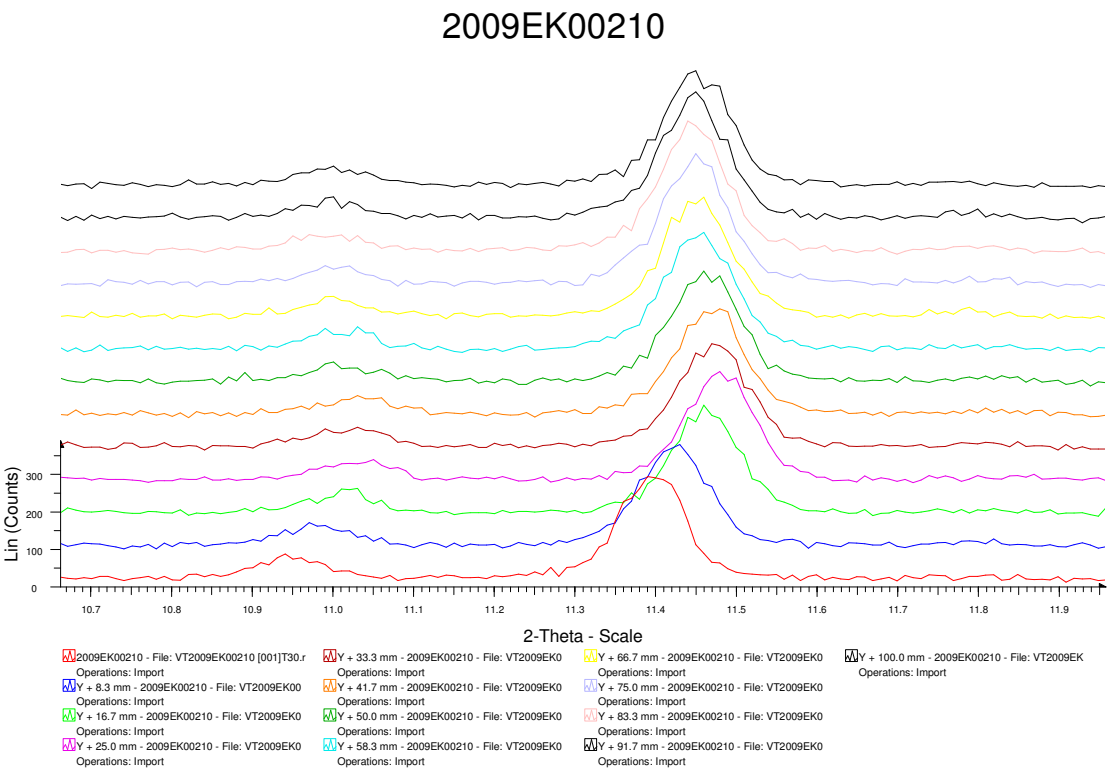

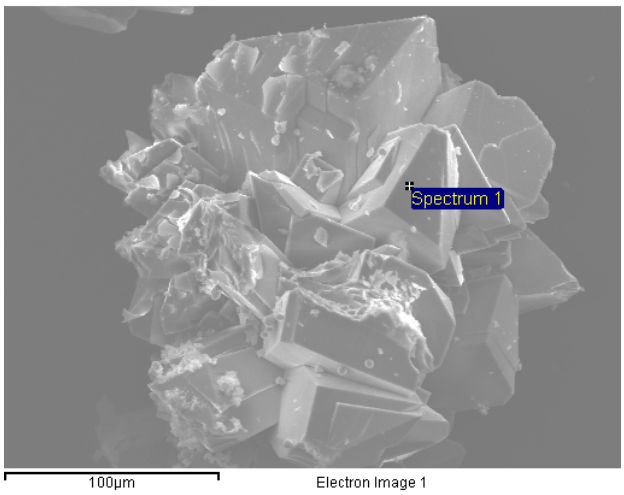

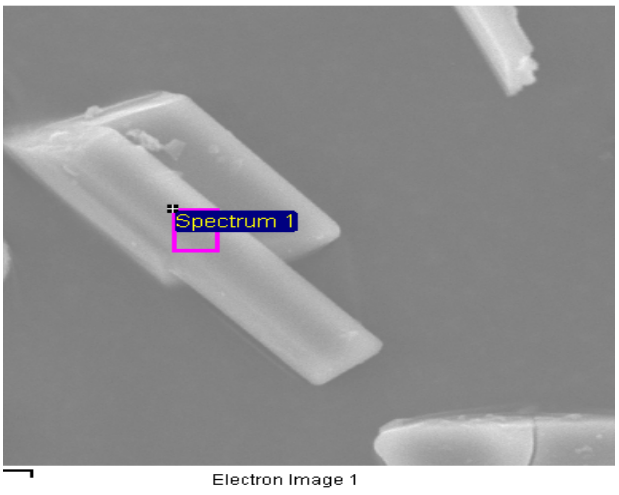

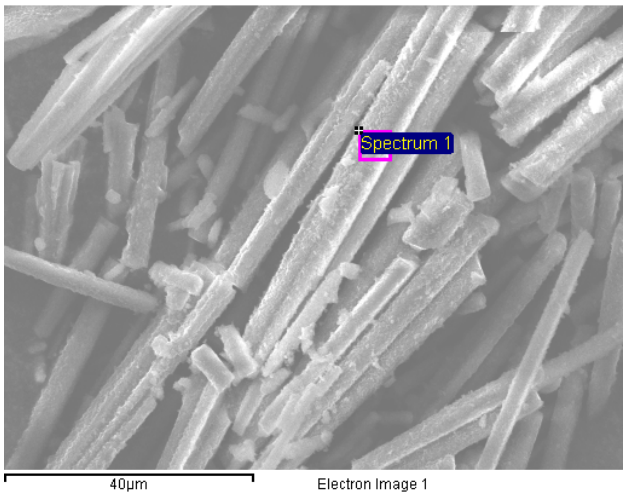

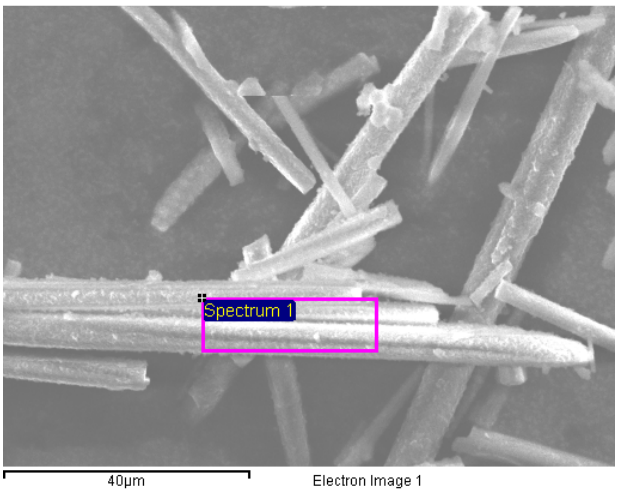

SEM micrographs for $[H_2N(C_2H_4)_2NH_2]_{1.5}[(VO)_2(AsO_4)F_2]O[(VO)(HAsO_4)F].H_2O$ **(1)** (top left), $[H_2N(C_2H_4)_2NH_2]_{1.5}[(VO)_3(AsO_4)F_4][VF_3(AsO_4)].4H_2O$ **(2)** (top right), $[\text{H-DABCO}]_x V_{72}As_{24}O_{204}F_{54}.nH_2O$,$\{[(VO)_3F_4(AsO_4)_{1+2/2}][V_2O_8F]_{1/2}[V_4O_4]_{1/2}\}_{12}$ **(3)** (bottom).

Table S10.1 : EDX data for Compound **(1)**

	V%	**As%**	**F%**	**V/As**	**V/F**
	18.64	13.39	21.46	1.392	0.868
	20.43	12.30	20.29	1.661	1.006
	22.48	14.13	21.51	1.591	1.045
Average	**20.52**	**13.27**	**21.09**	**1.546**	**0.973**

Calculated values based upon chemical formula: V:As:F = 1:1.5:1

Table S10.2: EDX data for Compound **(2)**

	V%	**As%**	**F%**	**V/As**	**V/F**
	21.84	11.96	Not able to determine;overlap with V	1.880	Note able to determine
	24.80	13.19		1.826	
Average	**23.32**	**12.58**		**1.854**	

Calculated values based upon chemical formula: V:As= 2:1

Table S10.3: EDX data for Compound **(3)**

	V%	**As%**	**F%**	**V/As**	**V/F**
	19.40	7.84	Not able to determine	2.47	Not able to determine
	19.70	7.04		2.80	
Average	**19.55**	**7.44**		**2.63**	

Calculated values based upon chemical formula [H-DABCO, H_2O, $(AsO_4)_y$ $]_x V_{72}As_{24}(O,F)_{258}$. nH_2O with y = 0, V:As= 3:1; for y> 1 values of V:As <3 are derived consistent with the measured value.

ESI.11 Comparison of calculated and experimental PXD patterns for compounds (**1**)- (**3**)

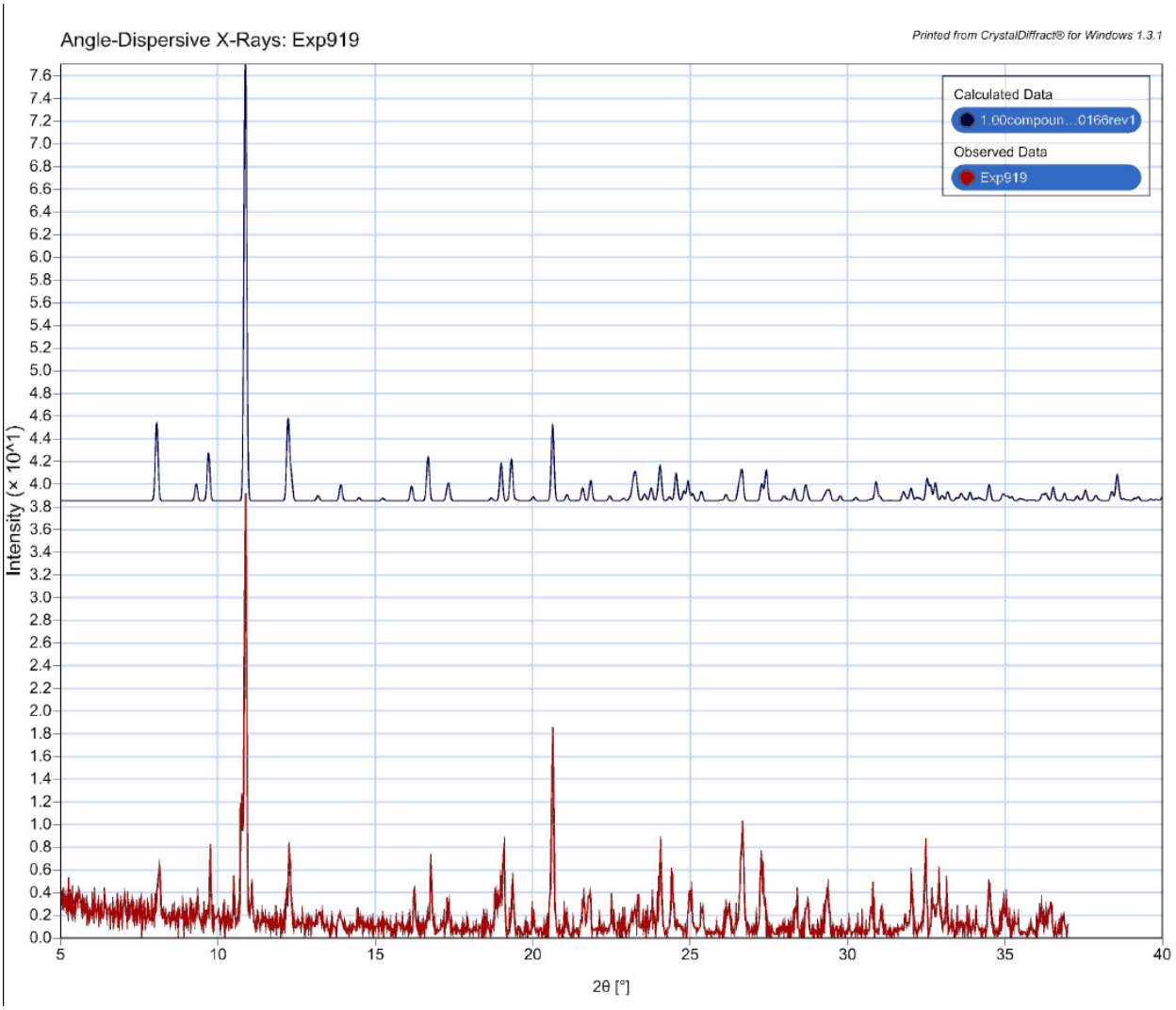

ESI11.1 Comparison of the calculated (upper profile) from SXD data and experimental (lower profile) PXD data plots for Compound **1** . Note that the calculated data used SXD coordinates and lattice parameters obtained at 120K while the experimental PXD data were collected at 298 K and thermal expansion is likely to cause a small shift in peak positions to lower 2theta values.

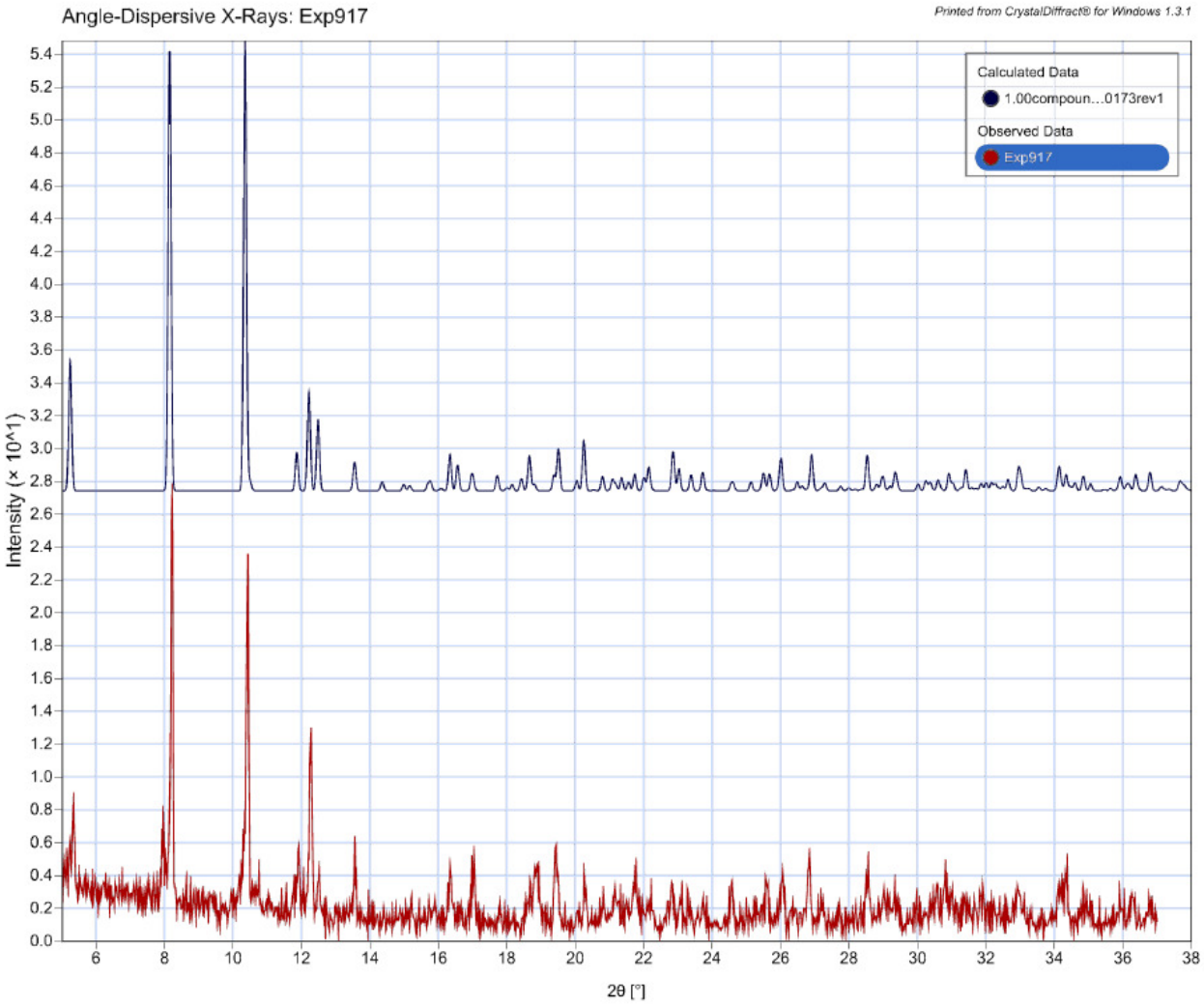

ESI11.2 Comparison of the calculated (upper profile) from SXD data and experimental (lower profile) PXD data plots for Compound **2** . Note that the calculated data used SXD coordinates and lattice parameters obtained at 120K while the experimental PXD data were collected at 298 K and thermal expansion is likely to cause a small shift in peak positions to lower 2theta values.

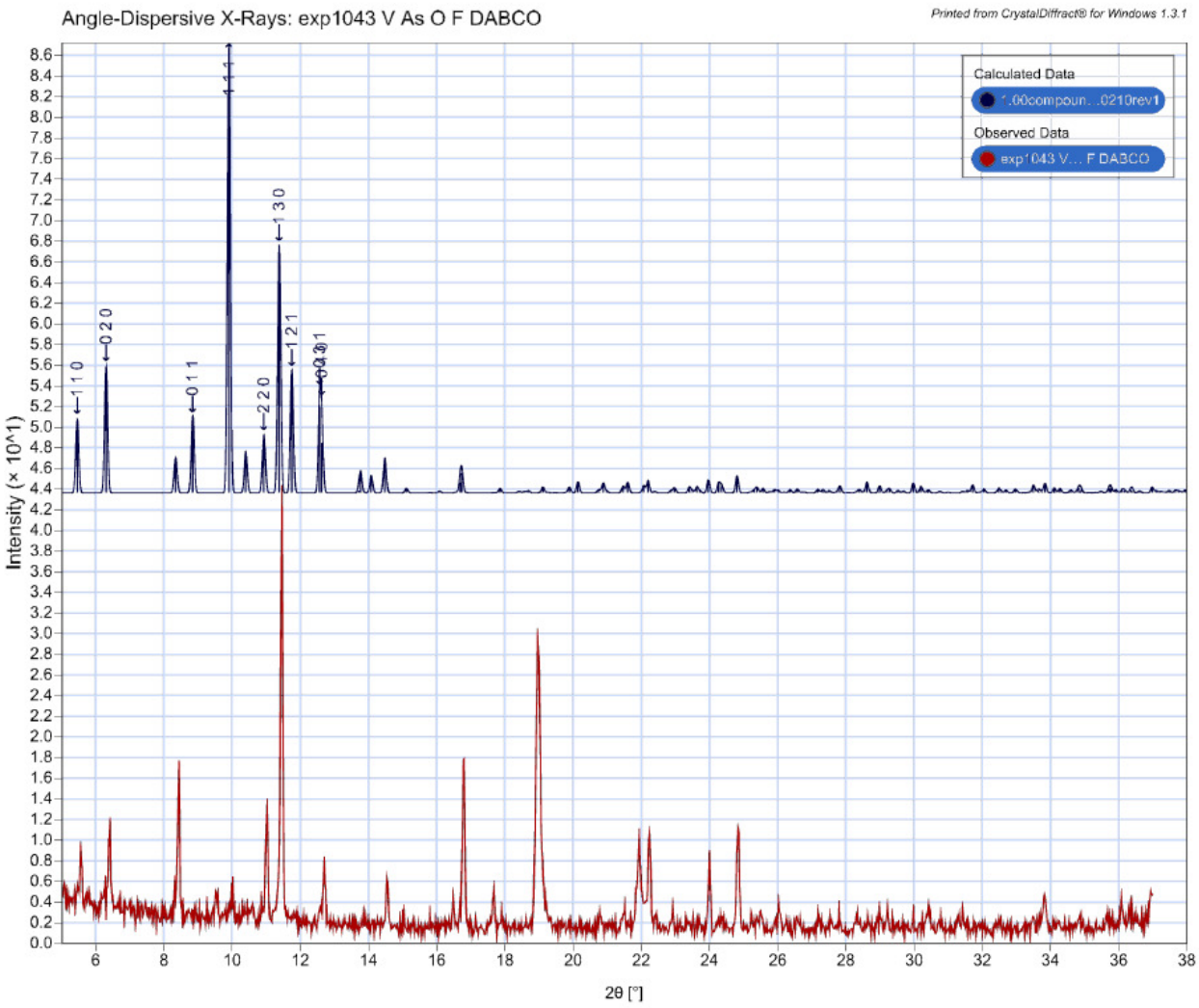

ESI11.3 Comparison of the calculated (upper profile) from SXD data and experimental (lower profile) PXD data plots for Compound **2** . Note that the calculated data used SXD coordinates and lattice parameters obtained at 120K while the experimental PXD data were collected at 298 K and thermal expansion is likely to cause a small shift in peak positions to lower 2theta values.

The experimental PXD data show strong preferred orientation along (hk0) making all reflections with l≠0, such as 111 much weaker.